CHICANE-FREE LASER HEATER SYSTEM FOR MITIGATION OF MICROBUNCHING INSTABILITY IN LINAC-FELS

F. Elisii[1], S. Di Mitri[2,*], G. Perosa[3]
[1] University of Trieste, Trieste, Italy
[2] Elettra Sincrotrone Trieste, Trieste, Italy
[3] European XFEL GmbH, Schenefeld, Germany

Abstract

We introduce a closed-form, verified through numerical integration, of the beam energy spread induced by oblique electron-laser interaction in a short undulator, so-called chicane-free laser heater. This scheme is relevant for high repetition rate free-electron lasers, space constrained, or subject to microbunching instability induced by a standard laser heater chicane. A calculation of the instability gain with the proposed scheme is presented to demonstrate its feasibility [1].

INTRODUCTION

In single pass or recirculating electron linear accelerators (linacs), microbunching instability (MBI) is the beam collective effect causing disruption or dilution of the longitudinal phase space by the amplification of energy and density modulations in succession [2]. The instability is seeded by the granularity of the electron distribution (shot noise), possibly in combination with narrowband phase space structures originated in radiofrequency (RF) photo-injectors [3,4]. The nature of the initial modulations, in combination with some damping mechanisms, commonly bounds the instability to final wavelengths in the range ~0.1–10's μm, hence the naming. Longitudinal damping of the instability is in most cases implemented through a laser heater system [5] in the low energy region of the linac, well before the instability builds up. In this case, the enlargement of the beam longitudinal emittance imposes a tradeoff between FEL spectral purity and intensity [6, 7].

At least three semi-analytical approaches to model MBI have been developed in the last two decades, which can be shortly referred to as, respectively, integral linearized Vlasov-Maxwell equation [8], matrix multiplication [9], and linearized Vlasov-Poisson equation in a plasma [10, 11]. We have recently upgraded the first two models [1], and translated them into Matlab scripts [12], finding excellent agreement in a wide variety of linac-FEL configurations and range of parameters. Here, we use one of the two to study beam heating in parallel *versus* oblique electron-laser interaction, the latter configuration being potentially relevant for very high repetition rate FELs, space constrained, or subject to instability development through the laser heater chicane.

Strictly speaking, the electron-laser interaction in the laser heater undulator does not require *per sé* a chicane, and the laser-induced energy modulation, in the range ~0.5–1 μm, can be translated into uncorrelated energy spread by smearing through the downstream magnetic bunch compressor. To the best of our knowledge, laser heater system at FLASH (Germany) is the only one implementing such scheme [13, 14]. However, a mini-chicane is still present upstream the undulator to inject the laser collinear to the electrons.

In the following, we evaluate the increase in laser peak power required by any pre-determined induced energy spread, in the presence of an oblique superposition (*e.g.*, in the horizontal plane) of laser and electrons. It is evident that the proposed scheme can, on the one hand, save several meters of space that would otherwise be occupied by the laser heater chicane. Moreover, it can offer a more efficient laser-electron interaction, thus a reduced laser power per induced energy spread, by virtue of smaller electron and laser beam spot size, owing to the absence of dispersive electron motion. On the other hand, the increase of peak power due to the larger effective interaction area has to remain compatible with the available average laser power, such as at superconducting linac-FELs requiring beam heating up to MHz repetition rate.

BACKGROUND

The energy modulation amplitude of an electron bunch induced by an external laser at an angle of interaction θ was derived in [15]. Equations 21–23 describing the induced energy modulation amplitude in that paper are recast here for the reader's convenience:

$$\Delta\gamma_{LH}(\theta) = \left(\frac{eE_0N_u\lambda_u}{m_ec^2}\right)\sqrt{I_x(L_u)I_y(L_u)}\cdot$$

$$\cdot\langle sin\left(-\varsigma + asin(2\varsigma) + dcos(\varsigma)\right)\cdot\left(o + psin(\varsigma) + qcos(2\varsigma)\right)\rangle_\varsigma \equiv$$

$$\equiv \left(\frac{eE_0N_u\lambda_u}{m_ec^2}\right)\Sigma_{JJ}(\theta) \qquad (1)$$

The following quantities have been introduced:

$$\begin{aligned}
\varsigma &= k_u z \\
a &= \frac{K^2}{4 + 2K^2 + 4\gamma^2\theta^2} \\
d &= \frac{k_s K sin\theta}{k_u\gamma} \\
o &= \left[\frac{1}{2\gamma^2}\left(1 + \frac{K^2}{2}\right) - 1\right] sin\theta \\
p &= -\frac{Kcos\theta}{\gamma} \\
q &= -\frac{K^2}{4\gamma^2} sin\theta
\end{aligned} \qquad (2)$$

*simone.dimitri@elettra.eu

$$I_{x,y}(L_u) = \frac{1}{L_u}\int_{-L_u/2}^{L_u/2} dz \frac{\sigma_L}{\sqrt{\sigma_{e(x,y)}^2(z) + \sigma_L^2(z)}}$$

where E_0 is the laser peak electric field, $L_u = N_u\lambda_u$ the number of undulator periods times the period length, z is the longitudinal coordinate internal to the bunch, $k_u = 2\pi/\lambda_u$, $k_s = 2\pi/\lambda_s$ the laser wavenumber, and K the undulator parameter planarly polarized. The correction factors $I_{x,y} \leq 1$ were introduced following [16] to describe the hourglass effect of laser and electron beam at a waist in the middle of the undulator.

The peak power P_L and the peak intensity I_L of a Gaussian laser pulse, whose transverse size at the waist is $w_0 = 2\sigma_L$, are:

$$P_L = \frac{1}{2} I_L \pi w_0^2 = \pi c \varepsilon_0 E_o^2 \sigma_L^2 \quad (3)$$

With the definition of $P_0 = \frac{4\pi c\varepsilon_0}{e^2}(m_e c^2)^2 = 8.7$ GW and from Eq.1, the RMS induced energy spread becomes:

$$\sigma_{E,LH}(\theta) = m_e c^2 \frac{\Delta\gamma_{LH}(\theta)}{\sqrt{2}} = m_e c^2 \frac{\sqrt{2}L_u}{\sigma_L}\sqrt{\frac{P_L}{P_0}}\sqrt{I_x I_y}\,\Sigma_{JJ}(\theta). \quad (4)$$

The evaluation of $\Sigma_{JJ}(\theta)$ through numerical integration implies some relevant computation effort in case of optimization studies, for which the overall MBI gain of the beam line is to be minimized as function of the beam, machine parameters and laser heater setting. For this reason, we provide below, as an alternative, a series representation. The mathematical passages are not reported here for the sake of brevity, and the Reader is kindly sent to [1] to review them. Here, we jump to the conclusions and show the agreement of the numerical integration and the proposed analytical form.

SERIES REPRESENTATION OF INDUCED ENERGY SPREAD

Let us introduce the following notation for the trigonometric terms in Eq. 1:

$$o\langle\ldots\rangle_o = o\cdot\langle\sin\big(-\varsigma + a\sin(2\varsigma) + d\cos(\varsigma)\big)\rangle_\varsigma$$
$$p\langle\ldots\rangle_p = p\cdot\langle\sin\big(-\varsigma + a\sin(2\varsigma) + d\cos(\varsigma)\big)\sin(\varsigma)\rangle_\varsigma \quad (5)$$
$$q\langle\ldots\rangle_q = q\cdot\langle\sin\big(-\varsigma + a\sin(2\varsigma) + d\cos(\varsigma)\big)\cos(2\varsigma)\rangle_\varsigma$$

and o, p, q are taken out from the integration (averaging) because independent from ς. Equation 5 is rewritten with Euler notation; $p\langle\ldots\rangle_p$ is taken hereafter as an example:

$$\langle\ldots\rangle_p = -\frac{1}{4}\langle e^{ia\sin(2\varsigma)}e^{id\cos(\varsigma)} - e^{-2i\varsigma}e^{ia\sin(2\varsigma)}e^{id\cos(\varsigma)} + +cc\rangle_\varsigma \equiv \frac{1}{4}[(\langle l\rangle - \langle t\rangle) + (\langle l^*\rangle - \langle t^*\rangle)] \quad (6)$$

The coupling term introduced in Eq.1 reads:

$$\sum_{JJ}(\vartheta) = -\frac{p}{2}\left[J_0^{-2,1}(a,d) + J_2^{-2,1}(a,d)\right] + \frac{q}{2}\left[J_1^{2,1}(a,d) - J_3^{-2,1}(a,d)\right] + o\cdot J_1^{-2,1}(a,d) \quad (7)$$

Since the index n of the infinite series in Eq.43 also determines the order of the Bessel functions, successive terms of the series will be smaller and smaller in value for higher n. The convergence of the series is, in fact, guaranteed already for $|n| = 4$ [1]. One should also be reminded that the dependence on the ϑ parameter is hidden in the arguments a, d of the Bessel functions. By dropping the interaction angle to zero, it returns as expected:

$$\sum_{JJ}(0) = \frac{K}{2\gamma}[JJ] \quad (8)$$

NUMERICAL RESULTS

Electron beam and laser heater parameters are inspired to [13]. In the absence of dispersive motion, we assume electron and laser beam sizes at the waist in the undulator squeezed to 100 μm and 150 μm respectively, see Table 1. The parameters allow beam heating in excess of 30 keV with 0.5 MW peak power for the collinear interaction. The maximum repetition rate assumed hereafter is 1 MHz.

Table 1. Laser Heater Parameters

Electron Bunch			
Mean energy	146		MeV
Normalized emittance, RMS	0.6		μm
Betatron function at the waist	5		m
Transverse rms size at the waist	100		μm
Charge	< 1		nC
Duration, FWHM	8		ps
LH-induced energy spread, RMS	< 30		keV
Undulator			
Period length	43		mm
Number of periods	11		
Undulator parameter *K*	1.43		
Laser Pulse			
Central wavelength	532	1064	nm
RMS size at the waist (x,y)	150		μm
Duration, FWHM	11		ps
Peak power at $\theta = 0$	< 0.50	< 0.12	MW
Average power at $\theta = 0$ & 1 MHz RR.	< 5.5	< 1.5	W

Figure 1 shows the dependence from the interaction angle of the LH-induced RMS energy spread at fixed peak power (top), and of the laser peak power at fixed induced energy spread of 30 keV (bottom). Two sets of undulator period are considered, to match the laser wavelength at the fundamental wavelength and at the 2nd harmonic, respectively (see Tab.1). The deviation of the series representation (Eq.7) and of the integral (Eq.1) is negligible for all angles, as also shown in Fig. 2, so confirming that our analytical derivation is exact.

At the interaction angle of 3 mrad, the maximum heating level of 30 keV can be obtained with 4 MW peak – 50 W average power at the second harmonic of the Yb-Nd laser, or at 1 MW peak–11 W average, for the laser at the fundamental harmonic (1.065 μm). The nominal peak power reported in [14] at the laser second harmonic is 2 MW.

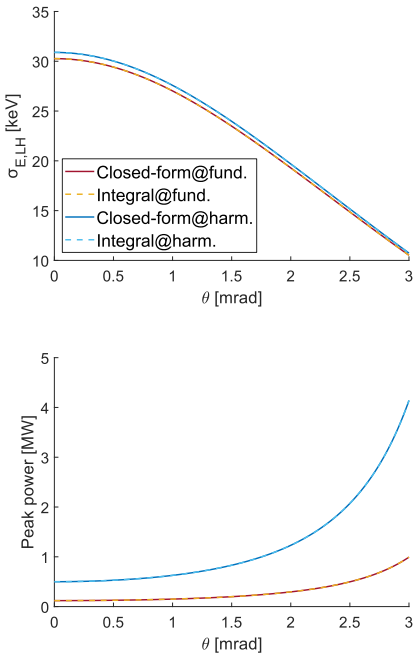

Figure 1. Laser heater-induced energy spread (top) and laser peak power (bottom) as function of the interaction angle. The laser heater is at the resonant condition at the fundamental and at the 2nd harmonic of the IR laser. Series representation and numerical integration superimpose.

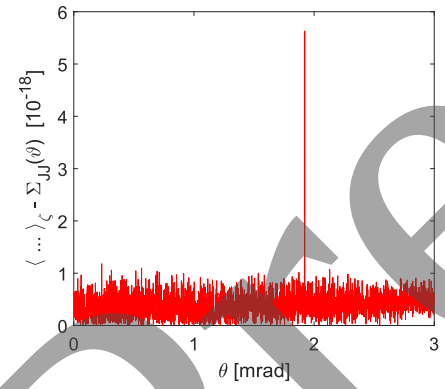

Figure 2. Numerical deviation of the series representation (Eq. 7) and of the numerical integration (Eq. 1), in unit of 10^{17}, as function of the interaction angle.

By keeping $\theta = 3$ mrad as the maximum tolerable angle for the laser power, and assuming a vacuum chamber iris radius of ~10 mm, the laser injection port should be approximately 4 m upstream the undulator. Assuming a laser RMS size of 150 μm at waist in the middle of the undulator, the laser spot size at the port would be 230 μm or 170 μm, at the fundamental or at the 2nd harmonic, respectively. Neither need of special focusing nor interference with the linac layout emerges at this stage.

To make a connection with the aforementioned comparative study, a 2-D map of the MBI gain of the 1.5 GeV linac, two-stage compression – whose gain is the largest among all four setups considered so far, see Fig. 8 – is produced in Fig. 3. The spectral gain is function of the laser heater peak power at the interaction angle of 3 mrad. The FERMI laser heater parameters are adopted [7]. The feasibility of the oblique interaction is confirmed in this case too.

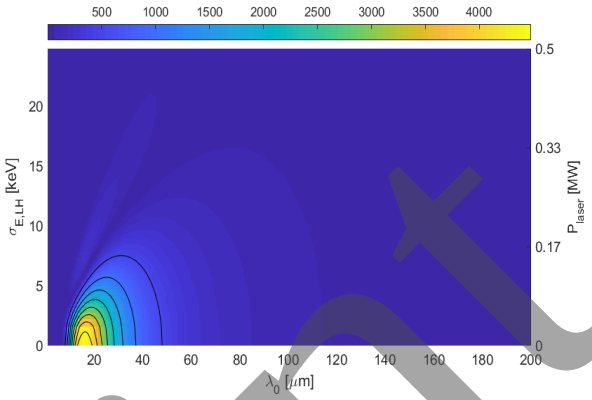

Figure 3. Contour plot of the spectral gain at the end of the 1.5 GeV, two-stage linac setting as function of the laser heater peak power. The induced energy spread is calculated for an interaction angle of 3 mrad.

CONCLUSIONS

The observed interaction of the laser heater chicane with the development of MBI at low energy suggests a scheme in which beam heating is implemented without a chicane. An approximated series representation for the energy spread induced by an obliquely incident laser is found and successfully compared to the numerical integration introduced in [13]. The study shows the feasibility of the oblique interaction in suppressing the instability for incident angles up to few mrad. In this case, the oblique interaction would save some meters of space along the linac axis, at the expense of a laser power 2 to 3-fold larger than in collinear laser-electrons geometry. In spite of the power increase, up to ~30 keV RMS energy spread can be induced at beam energies <200 MeV by an IR laser average power <50 W, up to MHz repetition rate.

REFERENCES

[1] S. Di Mitri, G. Campri, F. Elisii, G. Perosa, and S. Spampinati, "Systematic and comprehensive comparison of two semianalytical models of microbunching instability," *Phys. Rev. Accel. Beams*, vol. 28, no. 4, Apr. 2025 . doi:10.1103/physrevaccelbeams.28.044401

[2] Z. Huang and G. Stupakov, "Control and application of beam microbunching in high brightness linac-driven free electron lasers," *Nucl. Instrum. Methods Phys. Res., Sect. A*, vol. 907, pp. 182–187, Nov. 2018. doi: 10.1016/j.nima.2018.02.030

[3] J. Wu , P. Emma, Z. Huang, C. Limborg, M. Borland, "Temporal profile of the LCLS photocathode ultraviolet drive laser tolerated by the microbunching instability," SLAC National Accelerator Laboratory, Menlo Park, CA, USA, SLAC-PUB-10430 / LCLS-TN-04-6, 2004.

[4] S. Bettoni *et al.*, "Impact of laser stacking and photocathode materials on microbunching stability in photoinjectors," *Phys. Rev. Accel. Beams*, vol. 23, no. 2, Feb. 2020. doi:10.1103/physrevaccelbeams.23.024401

[5] E. L. Saldin, E. A. Schneidmiller, and M. V. Yurkov, "Longitudinal space charge-driven microbunching instability in the TESLA Test Facility linac," in Free Electron Lasers 2003, Ed., 2004, pp. 355–359. doi:10.1016/b978-0-444-51727-2.50081-x

[6] Z. Huang *et al., "*Measurements of the Linac Coherent Light Source laser heater and its impact on the x-ray free electron laser performance," *Phys. Rev. Accel. Beams,* vol 13, pp. 020703, Feb. 2010. doi:10.1103/PhysRevSTAB.13.020703

[7] S. Spampinati *et al.,* Laser heater commissioning at an externally seeded free-electron laser, *Phys. Rev. Spec. Top. Accel. Beams* vol. 17, pp. 120705, Dec. 2014.

[8] Z. Huang and K.-J. Kim, "Formulas for coherent synchrotron radiation microbunching in a bunch compressor chicane," *Phys. Rev. Spec. Top. Accel. Beams* vol. 5, no. 7, Jul. 2002. doi:10.1103/physrevstab.5.074401

[9] R. A. Bosch, K. J. Kleman, and J. Wu, "Modeling two-stage bunch compression with wakefields: Macroscopic properties and microbunching instability," *Phys. Rev. Spec. Top. Accel. Beams*, vol. 11, no. 9, Sep. 2008. doi:10.1103/physrevstab.11.090702

[10] A. Marinelli, E. Hemsing, and J. B. Rosenzweig, "Three-dimensional analysis of longitudinal plasma oscillations in a thermal relativistic electron beam," *Phys. Plasma*, vol. 18, no. 10, Oct. 2011. doi:10.1063/1.3638139

[11] V. N. Litvinenko *et al.*, "Plasma-cascade instability," *Phys. Rev. Spec. Top. Accel. Beams* vol 24, pp. 014402, Jan. 2021. doiL10.1103/PhysRevAccelBeams.24.014402

[12] The MathWorks, Inc. (2022). MATLAB version: 9.13.0 (R2022b).

[13] C. Gerth *et al.*, "Layout of the Laser Heater for FLASH2020+", in *Proc. IPAC'21*, Campinas, Brazil, May 2021, pp. 1647-1650. doi:10.18429/JACoW-IPAC2021-TUPAB111

[14] D. Samoilenko *et al.*, "First beam heating with the laser heater for FLASH2020+", in *Proc. IPAC'23*, Venice, Italy, May 2023, pp. 1950-1953. doi:10.18429/JACoW-IPAC2023-TUPL098

[15] X. Wang, C. Feng, C.-Y. Tsai, L. Zeng, and Z. Zhao, "Obliquely incident laser and electron beam interaction in an undulator," *Phys. Rev. Accel. Beams*, vol. 22, pp. 070701, July 2019. doi:10.1103/PhysRevAccelBeams.22.070701

[16] S. Di Mitri *et al,,* "Laser-slicing at a low-emittance storage ring," *J. Synchrotron Rad*., vol. 26, pp. 1523–1538, Sept. 2019. doi:10.1107/S1600577519009901